JOURNAL OF OPTOELECTRONICS AND ADVANCED MATERIALS, Vol. 11, No. 9, September 2009, p. 1044 - 1052

Origin of photoluminescence in tetrahedrally-bonded amorphous semiconductors and amorphous chalcogenides♣

TAKESHI AOKI*
Joint Research Centre of High-technology, Graduate School of Electronics, Tokyo Polytechnic University, Atsugi 243-0297, Japan

Using wideband quadrature frequency resolved spectroscopy (QFRS) expanded for lifetime measurement from 2 ns to 160 s, we have revealed that the lifetime distribution of the photoluminescence (PL) of a-Si:H is a triple-peak structure having the third peak at a lifetime ≥ 0.1 s, instead of the well-known double peaks at ~μs and ~ms. Moreover, the triple-peak phenomenon has been found to occur universally among non-crystalline semiconductors such as a-Ge:H and a-SiN:H, and chalcogenide glasses. The dependences of the QFRS spectra on temperature, excitation intensity and energy, emission energy and magnetic fields have elucidated that both *geminate* or *excitonic* recombination and *non-geminate*, or *distant pair* (DP) recombination co-exist in PL of non-crystalline semiconductors, which has settled the controversy as to whether the recombination is *germinate or non-geminate* in the PL. Observing the residual PL decay together with the QFRS in a-Si:H, we have also resolved the long-standing disagreement between the PL and light-induced electron spin resonance (LESR) signal. In addition, the paper presents the different effects of electric field on the two types of recombination.

(Received November 5, 2008; accepted December 15, 2008)

Keywords: Exciton, Radiative transition time, Geminate and nongeminate (DP) recombination, LESR, Effective temperature

1. Introduction

Research on recombination of photoexcited carriers in non-crystalline semiconductors is important for their application to optoelectronic devices such as solar-cells, light sensors and light emitters. Since photoluminescence (PL) is caused by radiative recombination of the photoexcited carriers, PL spectroscopy is a popular, relatively simple and well-established tool for studying the recombination mechanisms. In addition to conventional measurements of the PL spectrum, measurement of the PL lifetime distribution provides us with important insights to reveal the recombination mechanisms. Quadrature frequency resolved spectroscopy (QFRS) of PL is effective in analysing the lifetime distribution at sufficiently low generation rates of photocarriers G, in contrast to time resolved spectroscopy (TRS) [1].

High-quality films of hydrogenated tetrahedrally-bonded amorphous Si (a-Si:H) are one of the rather easily obtainable and important materials for optoelectronics applications. A salient feature of a-Si:H is the existence of an intrinsic distribution of band-tail localized states, which strongly influence the electronic and optical properties.

The two types of recombination of an electron-hole (e-h) pair can be considered in the PL of a-Si:H, as well as other amorphous semiconductors at low temperatures, T. One is *geminate* recombination, where an e-h pair is created by a photon of energy exceeding the band-gap and mutually coupled by a Coulomb attractive force. In geminate recombination, the Coulombic effect allows the pair to recombine within itself. In particular, a *geminate* e-h pair having a hydrogen-like system is called an *exciton*, which is classified into two electronic states; *singlet* (S = 0) and *triplet* (S = 1) according to the total spin S of the e-h pair.

The other is *non-geminate*, or *distant-pair* (DP) recombination, where an electron escapes from its partner hole of an e-h pair created by the identical photon and can recombine with a hole created by another photon. While e-h pairs with energies exceeding the band edges for band-to-band excitation relax to the band edges via thermalization and hop down into the band-tail localized states, some of them split into electrons and holes, which randomly distribute themselves in the localized states. The

♣ Paper presented at the International School on Condensed Matter Physics, Varna, Bulgaria, September 2008

DP recombination occurs preferentially for a pair with the shorter e-h distance r with a recombination lifetime τ given by the radiative tunnelling (RT) model at low T,

$$\tau = \tau_O \exp(2r/a) \quad (1)$$

where τ_O is radiative electric dipole transition time of the order of 1 ~ 10 ns and a is the larger extent of either the electron or hole wave-function, being a localized electron radius of ~1 nm in the case of a-Si:H [2].

Exciton involvement in the PL of a-Si:H at low temperatures was once suggested [3,4]. Probably owing to the disorder of amorphous materials in contrast to crystalline ones, however, excitonic absorption spectrum has not been observed except for a-SiO_2. Therefore, the PL in a-Si:H, whether it is geminate or non-geminate, has been often interpreted in terms of the RT model [2]. In contrast, the PL of a-As_2S_3 and a-As_2Se_3 has been frequently interpreted in terms of the exciton model. Thus, in a-Si:H, the main emphasis has been placed for a long time rather on a controversy as to whether the PL originates from geminate or non-geminate (DP) recombination.

Using QFRS to measure the PL lifetime distributions, Bort *et al.* [5] discovered a geminate condition at the generation rate $G \approx 10^{19}$ cm^{-3} s^{-1} in a-Si:H, below which the peak lifetime τ_T (~ms) is independent of G and thus the metastable or steady-state photocarrier density $n_T = G\tau_T$ is *proportional* to G. Above the geminate condition $G > 10^{19}$ cm^{-3} s^{-1}, τ_T decreases with increasing G, which is interpreted by the DP recombination with the RT model. Hence the sub-linear dependence of $n_T = G\tau_T$ on G is predicted at $G > 10^{19}$ cm^{-3} s^{-1}.

However, the intensity of the light-induced electron spin-resonance (LESR), analogous to n_T, is known to be sub-linearly dependent on G approximately as $\propto G^{0.2}$ in the whole range of G from 10^{13} to 10^{23} cm^{-3} s^{-1} [5-7]. The DP recombination model successfully predicts this sub-linear G-dependence of the LESR intensity, but it fails to explain the linear dependence of n_T on G below the geminate condition, where the lifetime τ_T is constant [8].

It has been already established by QFRS that the PL lifetime distribution is double-peaked in a-Si:H, consisting of short-lived (~μs) and long-lived (~ms) components under the geminate condition. However it is difficult to identify the two lifetime components on the basis of the RT model [9,10]. Stachowitz *et al*. [11] proposed exciton involvement in the double peak phenomena, attributing the short- and long-lived components to a singlet (S = 0) exciton and triplet (S = 1) exciton, respectively.

Developing the wideband QFRS technique which allows analysis of lifetimes over almost 11 decades from 2 ns to 160 s, we observed double-peak lifetime behaviour in not only tetrahedrally-bonded a-Ge:H and a-SiN:H but also amorphous chalcogenides, e.g. g-As_2S_3 and a-Se, and supported the exciton model [12-14].

The wideband QFRS also revealed that the lifetime distribution is triple-peaked, accompanied by a third lifetime peak in the long lifetime range of 0.1 ~ 160 s in the PL of a-Si:H and a-Ge:H under the geminate condition. The third component exhibited characteristic features of the DP recombination [15]. Thus, we claimed that *geminate recombination* and *non-geminate* (DP) *recombination co-exist* in the PL of a-Si:H and a-Ge:H even under the geminate condition at low T and low G. Moreover, a similar phenomenon was observed in chalcogenide amorphous semiconductors, indicating that the triple-peak QFRS spectrum, i.e., the *co-existence of geminate and non-geminate recombination*, is universal among amorphous semiconductors [16-18].

Moreover, PL recombination for lifetimes longer than 160 s was investigated by observing the residual PL decay after cessation of PL excitation in a-Si:H at low G [19]. This very long-lasting PL decay, as well as the DP component of QFRS spectra, resolves the long-standing controversy concerned with the G-dependences of the steady-state photo-generated carrier density in the PL and the LESR intensity [15,19,20].

The present paper reviews our previously published results, demonstrating both excitonic recombination and DP recombination in PL of undoped a-Si:H and other amorphous semiconductors. We also claim that the residual PL decay persisting for more than ~10^4 s reflects the decay kinetics of the DP recombination and consistency with the LESR results. The paper also presents the difference of the electric-field effect on the PL between the geminate or excitonic recombination and the DP recombination in a-Si:H [21,22].

2. Coexistence of geminate recombination and non-geminate recombination

2.1 Triple-peak lifetime distribution

Fig. 1 shows QFRS spectra of a-Si:H from 2 ns to 160 s excited at the PL excitation energy E_X = 2.33 eV for various generation rates G, from 2.5×10^{15} to 5.0×10^{22} cm^{-3}s^{-1} [20]. We can see that the long- and short-lived components are fixed at $\tau_T \approx 4$ ms and at $\tau_S \approx 2$ μs, respectively, even though G changes from 2.5×10^{15} to 4.1×10^{19} cm^{-3} s^{-1}. This is the well-known double-peak lifetime distribution observed under the so-called geminate condition $G \le 10^{19}$ cm^{-3}s^{-1} [9,10].

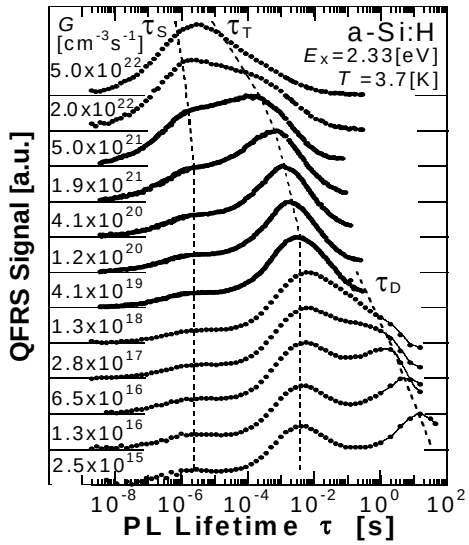

Fig.1 QFRS spectra from 2 ns to 160 s for a-Si:H at 3.7 K and E_X =2.33 eV with various G[20].

However, a new third peak higher than the other two is observed at $\tau_D \approx 20$ s for $G \approx 2.5\times10^{15}$ cm^{-3}s^{-1}, which might have been overlooked earlier due to the lack of the very low frequency QFRS.

As G increases, τ_D continuously shifts to shorter lifetimes and the peak merges with the τ_T- component at $G \approx 1.3\times10^{18}$ cm^{-3}s^{-1}. The continuous shortening of τ_D with increasing G is a distinctive feature of the DP recombination based on Eq. (1) of the RT model and the plot of τ_D vs. G fits well the curve calculated from the balance equation [23]. Thus, the PL lifetime distribution of an intrinsic a-Si:H is triple-peaked at a low T of 3.7 K under the geminate condition $G \leq 10^{19}$ cm^{-3}s^{-1}. At sufficiently low G, the three peaks possess well-separated lifetimes, suggesting that the recombination events at τ_S, τ_T and τ_D occur via three independent, or non-competing recombination channels.

Similar triple-peaked lifetime structures are also observed in the G-dependent QFRS spectra of a-Ge:H excited at E_X = 1.81 eV and T = 3.7 K under the geminate condition $G \approx 10^{19}$ cm^{-3}s^{-1} [15]. We have also observed the DP component in a-SiN:H [13] and chalcogenides such as g-As_2S_3, a-As_2Se_3, a-Se and g-GeGaSe [16-18], as well as the double-peaks at τ_S and τ_T except for a-As_2Se_3 [14, 24]. However, the DP component is less pronounced and its dependence on G is rather indistinguishable in these amorphous semiconductors, which is due to the competing non-radiative recombination via defects [13].

Fig. 2(a) demonstrates the triple-peaked QFRS spectra of GeGaSe chalocogenide glass for various emitted photon energies $\hbar\omega$, showing the triple peaks at τ_S, τ_T and τ_H. The third peak located at a lifetime $\tau_H \approx 20$ s arises from the DP recombination, which is strongly influenced by the non-radiative recombination via defects, exhibiting a very weak dependence of τ_H on G and E_X [17,18].

Fig. 2(b) demonstrates the quantum efficiencies (QEs) η_S, η_T and η_H corresponding to the τ_S-, τ_T- and τ_H-components obtained by deconvoluting the QFRS spectra (a) as functions of $\hbar\omega$, i.e., the PL spectra of the individual recombination events. The peak energy of the τ_S-component ~1.02 eV is higher by ~80 meV than that of the τ_T-component ~0.94 eV. This suggests that the exchange energy E_{ex} between the singlet exciton (τ_S-component) and the triplet exciton (τ_T-component) is ~80 meV, in contrast to $E_{ex} \approx 40$ meV for a-Si:H [25].

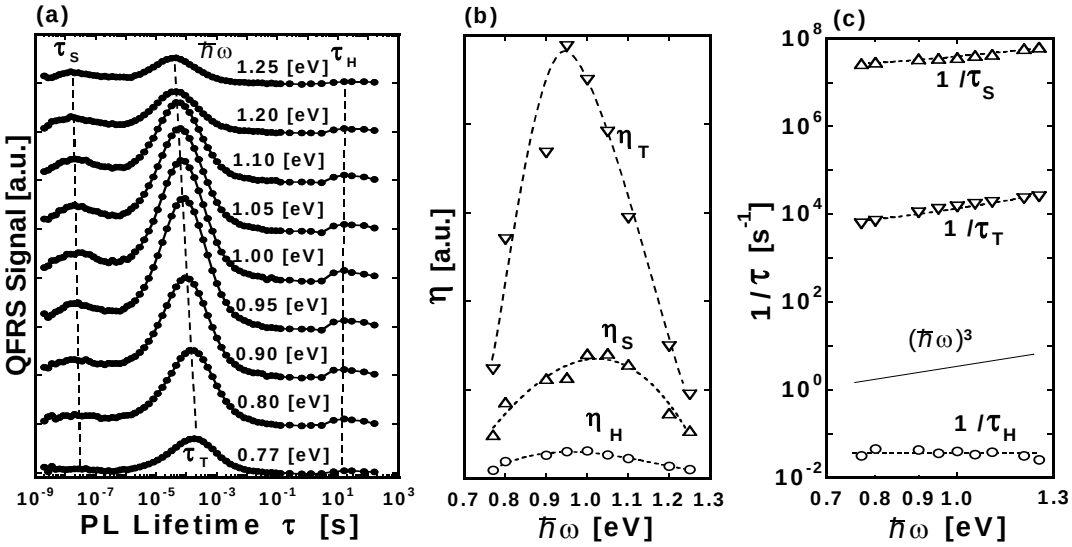

Fig.2 (a) PL emission energy $\hbar\omega$-evolved QFRS spectra of undoped g-GeGaSe at E_X = 2.33 eV, T = 3.7 K and $G \approx 10^{20}$ cm^{-3}s^{-1}. (b) The three components of (Δ) η_S, (▽) η_T, (○) η_H deconvoluted from (a) as functions of $\hbar\omega$, i.e., the PL spectra of QEs η_S, η_T and η_H. (c) Radiative recombination rates (Δ) $1/\eta_S$, (▽) $1/\eta_T$ and (○) $1/\eta_H$ of the three components plotted against $\hbar\omega$ on a log-log scale [18].

Fig. 2(c) shows the recombination rate τ^{-1} of each component as a function of $\hbar\omega$ on a log-log scale. The recombination rates τ_S^{-1} and τ_T^{-1} roughly depend on $\hbar\omega$ as $\propto (\hbar\omega)^3$, which supports that the τ_S- and τ_T-components are ascribed to the excitonic recombination process as those of a-Si:H [19,25]. On the other hand, the recombination rate τ_H^{-1} is almost independent of $\hbar\omega$. This suggests that the τ_H component should be ascribed to the DP recombination of photoexcited carriers after hopping down in band-tail states [16-19].

2.2 Excitonic recombination

The singlet exciton lifetime τ_S, the triplet exciton lifetime τ_T and the spin-exchange energy E_{ex} obtained by QFRS are tabulated for various amorphous semiconductors in Table 1. We can see that τ_S widely ranges from 10 ns, being close to the

Table 1. Singlet (τ_S) and triplet (τ_T) exciton lifetimes and spin-exchange energy (E_{ex}) for various amorphous semiconductors.

	τ_S (μs)	τ_T (ms)	E_{ex}(meV)
a-Si:H	2	4	40
a-Ge:H	20	0.8	—
a-SiN:H	0.01	1	50 ~180
g-As_2S_3	0.01	0.1	100
a-As_2Se_3	—	0.8	—
a-Se	0.2	1	160
g-GeGaSe	0.02	0.1	80

electric-dipole transition time τ_O, to 20 μs for the various materials. This can be explained by invoking self-trapped excitons (STEs), as follows [24-27].

After excitation of an e-h pair in a-Si:H, a hole of the pair will be immediately self-trapped as the self-trapped hole (STH) with a radius a_h in a deeply-localized state of the valence-band-tail having a higher density of states, while its partner electron is rather free owing to the lower density of conduction-band-tail states. The electron will be loosely-bound to the STH by Coulomb attraction, forming a STE rather than trapped to a localized state of the conduction-band-tail. Thus the STE has a Bohr radius a_B* larger than the electron localization radius in the conduction-band-tail a usually ~1 nm for a-Si:H. The discrepancy in the orbital size between the initial state (a_B*) and the final sate (a_h) reduces the radiative transition rate of the singlet STE by an amount $(a_h/a_B^*)^3$ [24-26].

Furthermore, the formation of the three lifetime components in amorphous chalcogenides has been interpreted on the basis of the Mott-Davis-Street (MDS) model [17,18,28].

Kivelson and Gelatt [27] gave the radiative transition rate τ_S^{-1} of the singlet exciton as

$$\frac{1}{\tau_S} = \frac{4}{3}\kappa^{1/2}\left[\frac{e^2}{\hbar c}\right]\left[\frac{\omega^3}{c^2}\right]a_h^{\,2}S \ , \qquad (2)$$

where κ is the static dielectric constant, $e^2/(\hbar c) \approx 1/137$ is the fine structure constant, $\hbar\omega$ is the emitted photon energy, c is the speed of light, and S is an overlap term given by $\sim(2a_h)^3/(a_B^*)^3$. If S is omitted from the right-hand side of Eq. (2), it is equal to the radiative electric-dipole transition rate τ_O^{-1} with an electric-dipole moment ea_h given by Wilson *et al*. [29]. Since a_B* for a-Si:H was estimated to be ~2.4 nm by Kivelson and Gelatt [27] and ~5 nm by us [20] as described in Section 2.3, we obtain τ_S ranging from ~1.2 to ~11 μs, with the photon energy $\hbar\omega$ = 1.5 eV, κ = 12 and a_h = 0.2 nm. As Eq. (2) has an order of magnitude uncertainty, our experimental result of $\tau_S \approx 2$ μs agrees quite satisfactorily with the estimated values. Lifetimes of the singlet and triplet excitons are calculated for amorphous semiconductors using different recombination models from that mentioned in Section 2.3 [30,31].

Wilson *et al*. observed $\tau_S \approx 10$ ns for a-Si:H by TRS [29]. As far as the author knows, however, there is no TRS of PL in a-Si:H *under the geminate condition* except for that of Stearns [32], where the PL decay $I(t)$ was non-exponential in the range of time t = 0.5 ~ 40 ns after PL excitation. The plot of $t \times I(t)$ as a function of log t gives an approximate lifetime distribution similar to the QFRS spectrum [1]. We show the QFRS spectrum of PL in a-Si:H at $\hbar\omega \approx 1.5$ eV and superimpose the plot of $t \times I(t)$ obtained from the Stearns' data in Fig. 3. This also proves the absence of a peak in the ns region of the TRS in the PL of a-Si:H *under the geminate condition* [24].

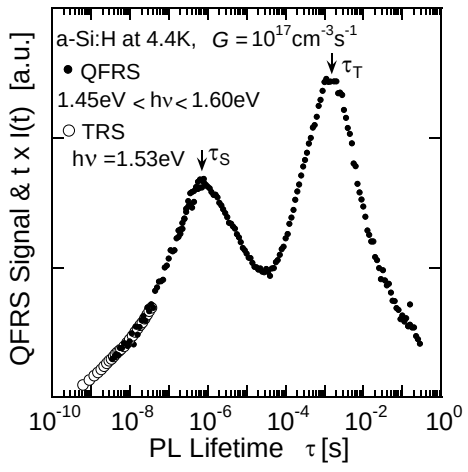

Fig. 3 (•) QFRS spectrum of PL with emission energy 1.45<hν <1.60 eV for a-Si:H under the geminate recombination condition $G \approx 10^{17}$ cm^{-3}s^{-1} at 4.4 K and E_X = 2.33 eV. (○) Plots of t×I(t) vs. $\log_{10} t$ obtained from Stearns' TRS data [24,32].

2.3 Steady-state photocarrier density of geminate and non-geminate recombination

Deconvoluting the QFRS spectra for various G in Fig. 1, we obtain the steady-state or metastable photocarrier densities of the three recombination components of PL in a-Si:H, i.e., $n_S = \eta_S G\tau_S$ (□), $n_T = \eta_T G\tau_T$ (▲) and $n_D = \eta_D G\tau_D$ (○) as functions of G as shown in Fig 4. It is a characteristic feature of geminate or excitonic recombination that the steady-state carrier densities n_S and n_T increase linearly against G, while the lifetimes τ_S and τ_T remain constant. On the other hand, with increasing G, τ_D decreases and thus $n_D = \eta_D G\tau_D$ increases sub-linearly with G, roughly as $n_D \propto G^{0.2}$.

The LESR spin density vs. G (Δ, ∇, •) obtained by other three groups is also plotted in Fig.4, which agrees with n_D vs. G (○) without any adjusting parameters [5,7]. This suggests that the LESR results reflect the DP recombination, which is discussed in more detail in Section 3.

The steady-state carrier concentration n_T of the τ_T-component increases almost in proportion to the generation rate G under the geminate condition $G \le 10^{19}$ cm^{-3}s^{-1} as reported in [5]. When G exceeds 10^{19} cm^{-3}s^{-1}, the plot of n_T merges with the sub-linear plot of $n_D \propto G^{0.2}$ at the steady-state carrier density $n_T \approx n_D \approx 10^{17}$ cm^{-3}. At $G \approx 10^{19}$ cm^{-3}s^{-1}, the triplet exciton component and the DP component can be seen merging in the QFRS spectra (Fig. 1). This implies that the recombination of the triplet exciton is prevailed over by that of DP at $n_T \approx 10^{17}$ cm^{-3}.

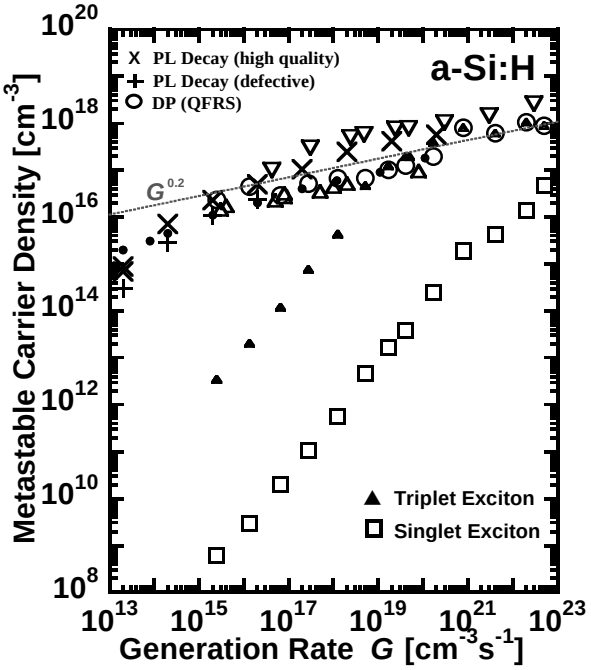

Fig. 4 Metastable carrier density n_{met} vs. generation rate G; × and + denote n_{met} deduced by integrating the PL decay for a high-quality film and a defective film of a-Si:H, respectively. The plots ○, □ and ▲ indicate the steady-state carrier densities n_D, n_S and n_T, respectively, obtained from the QFRS spectra in Fig.1., and • denote the LESR densities obtained from [5], [6] and [7], respectively. The unit of the plots of is arbitrary [6]. The straight line indicates $n_{met} \propto G^{0.2}$.

Similarly, an extrapolation of the plot of n_S vs. G intersects with the sub-linear plots at around $n_S \approx n_D \approx 10^{18}$ cm^{-3} ($G \approx 10^{23} \sim 10^{24}$ cm^{-3}s^{-1}), though it deviates from a straight line above $G \approx 10^{21}$ cm^{-3}s^{-1} owing to the irradiation condensed by a lens. Such a coalescence of all the components is also seen at $G \approx 5.0\times10^{22}$ cm^{-3}s^{-1} in Fig. 1.

If the triplet excitons are assumed to be transformed to DPs at the point of coalescence with $n_T \approx n_D$, the average e-h distance of the DPs given by $\sim 0.5 n_T^{-1/3}$ is estimated to be ~10 nm by $n_T \approx n_D \approx 10^{17}$ cm^{-3}. This suggests that the Bohr radius of the triplet excitons is close to ~10 nm. Similarly, at the coalescence of the singlet excitons and DPs at around $n_S \approx n_D \approx 10^{18}$ cm^{-3} the average e-h distance $\sim 0.5 n_S^{-1/3}$ amounts to ~5 nm [20]. Thus a singlet exciton radius a_B* is considered to be close to ~5 nm and then the exciton binding energy $e^2/2\kappa a_B$* works out to be ~5 meV with a dielectric constant $\kappa \approx 12$, which explains the disappearance of the τ_S- component at low $T \approx$ 30 K [20].

Fig. 5 illustrates a model of PL in a-Si:H composed of three lifetime components, i.e., a singlet exciton (τ_S), a triplet exciton (τ_T) and a DP (τ_D) [1,13]. It should be noted that the excitonic recombination model shown here is different from the previous one [33]. The larger exchange energy $E_{ex} \approx$ 40 meV than the binding energy of singlet exciton is probably attributable to localization of STEs [1,20].

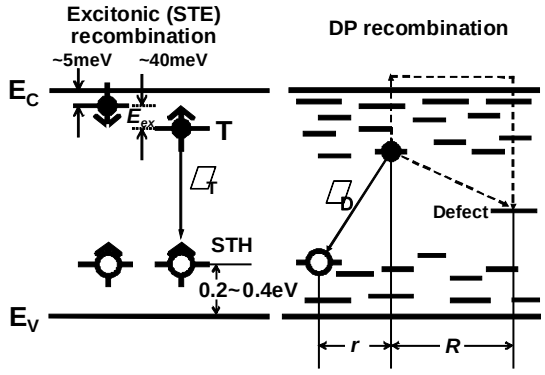

Fig.5 Recombination model of a-Si:H consisting of

singlet (τ_S) and triplet (τ_T) self-trapped excitons (STE) and distant-pairs (DP(τ_D)) with e-h pair separation r. The exchange energy $E_{ex} \approx 40$ meV and singlet-exciton binding energy ~5 meV are obtained in [25] and [20] respectively. The electron of the DP has a distance R to a defect. Thin solid arrows indicate radiative recombination. An oblique dotted arrow indicates non-radiative tunnelling and vertical one to the defect indicates non-competing non-radiative recombination. Thick arrows indicate spins of electrons and holes [13].

The PL model of amorphous chalcogenides is given on the basis of the MDS model in our previous papers [17,18].

3. Consistency between metastable PL carrier density and LESR intensity.

Fig. 6 shows log-log plots of PL intensity $I(t)$ vs. time t after cessation of PL excitation of 2.33 eV, i.e., $\log_{10}I(t)$ vs. $\log_{10}t$ for various values of G from 10^{13} to 10^{19} $cm^{-3}s^{-1}$ taken for a-Si:H at 3.7 K. Except for the lowest G value of 2×10^{13} $cm^{-3}s^{-1}$, the PL decay curves converge asymptotically at long times of $\sim 10^4$ s, even though they are initially different by 5 orders of magnitude. Since excitonic or geminate recombination affects the early stage of the PL decay at times $t < 1$ s, we have fitted each curve, at times long enough after switching off the PL excitation, to the derivative of a stretched exponential (SE) function expressed as $Kt^{\beta-1}\exp[-(t/\tau_0)^{\beta}]$, which is derived from a time-dispersive rate equation for monomolecular reactions. Here, τ_0 is the effective recombination time and β is a dispersion parameter ($0 < \beta < 1$). The fact that the PL decay $I(t)$ fits $Kt^{\beta-1}\exp[-(t/\tau_0)^{\beta}]$ for various values of G ($\leq 2\times10^{19}$ $cm^{-3}s^{-1}$) and T can be considered to be a manifestation of a time-dispersive monomolecular reaction in the DP recombination, for the reason described in [19].

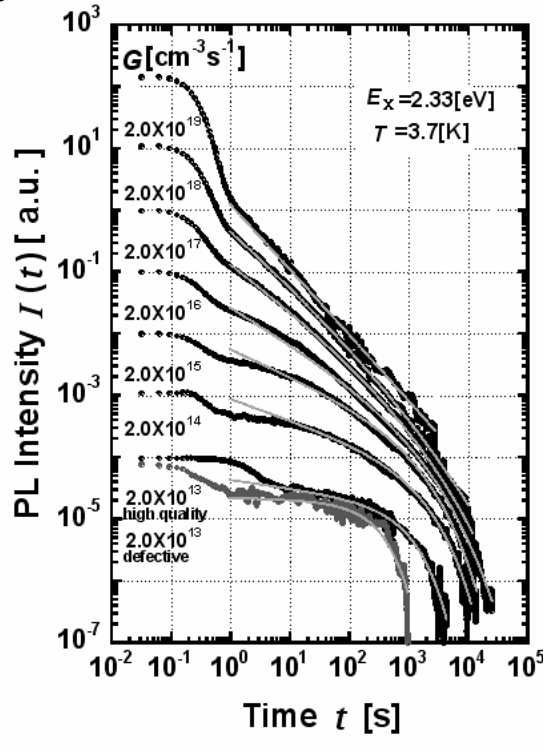

Fig.6. Log-log plots of PL decay I(t) of a high-quality a-Si:H film with various values of G at 3.7K. The plots are fitted to the derivative of the SE functions (half-tone curves). The plots in half-tone are for a defective film at $G = 2\times10^{13}$ $cm^{-3}s^{-1}$ [19].

Morigaki [34] estimated β and τ_0 by fitting the LESR intensity decay obtained by Yan et al. [7] to the SE function for various G. In Fig. 7(a), the error bars show β vs. G obtained from the PL decay $I(t)$ of Fig. 6 and the squares (□) show β vs. G obtained by Morigaki from the LESR intensity decay [34]. Similarly in Fig. 7(b), the error bars show τ_0 vs. G obtained from the PL decay and the squares (□) show τ_0 vs. G obtained from the LESR intensity decay [34].

We adopted the non-linear least square fit programme of *Origin* 7J and the non-linear regress of the statistic package of *Mathematica* ver. 4 to fit the data to $Kt^{\beta-1}\exp[-(t/\tau_0)^{\beta}]$. The lengths of the error bars indicate the extents of β and τ_0, in which the non-linear least square fit keeps the value of chi-squared within 1.5 times its minimum value.

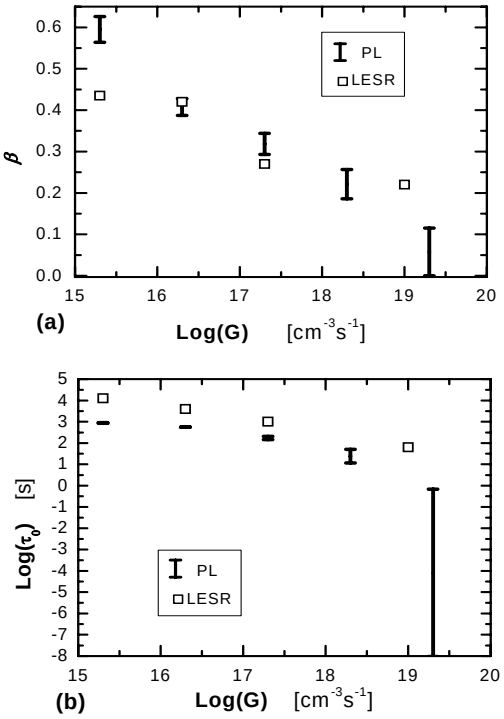

Fig.7 (a) *β vs. G,* (b) *τ_0 vs. G. The error bars from the PL decay of Fig. 6, squares (□) were obtained by Morigaki from the LESR decay [34].*

In Figs. 7(a) and (b), we notice that τ_0 as well as β shows a very similar tendency in two different decay-measurements, i.e., the PL decay and the LESR intensity decay. The difference of an order in magnitude of τ_0 between the PL decay and the LESR decay is explained as follows.

Firstly, the measuring time t is very different between the two measurements; the PL decay was measured for $t > 10^4$ s except for $G = 2 \times 10^{19}$ cm^{-3} s^{-1}, whereas the LESR decay was measured only up to $t = 2 \times 10^3$ s [7]. Since τ_0 is relevant at long times, a short measuring time will lead to noticeable error. Actually, the PL decay at $G = 2 \times 10^{19}$ cm^{-3}s^{-1} was measured only to $t \approx 2.7 \times 10^3$ s (Fig. 6), and thus τ_0 contains a considerable error, as shown by the longest error bar at $G = 2 \times 10^{19}$ cm^{-3}s^{-1} in Fig. 7(b).

Secondly, the temperature is different between the two measurements. The PL decay was measured at 3.7 K, whereas the LESR decay was measured at 40 K, where the hop-up of electrons localized in band-tail states is no longer negligible; it enhances the DP recombination as well as the hopping transport [21,35]. In fact, at $T = 40$ K, τ_D is shortened and η_D is increased as described in Section 4, and furthermore n_D as well as the LESR density decreases to ~1/3 of that at a low T [15,20]. Therefore, the temperature difference changes the kinetics of decay, resulting in the different values of β and τ_0 between the two decay phenomena.

Thirdly, the PL decay was excited at 2.33 eV, whereas the LESR decay was excited at 1.96 eV. This might have introduced an error of one order of magnitude in G, since G is proportional to the absorption coefficient, which changes widely in the range of these photon energies.

Finally, τ_0 is calculated according to the form $A^{1/\beta}$ with one of parameters, A, coming from the non-linear least square fit, so that the error in τ_0 increases with decreasing β.

The integration of $I(t)$ from $t = 0$ to ∞ is proportional to the metastable carrier density n_{met} at a continuous excitation rate G [19]. We plotted n_{met} (×) against G in Fig. 4, where the proportionality constant between the integral of $I(t)$ and n_{met} is calculated by adjusting n_{met} to n_D at $G = 2 \times 10^{16}$ cm^{-3}s^{-1}. Both n_{met} and n_D show sub-linear G-dependences ($\propto G^{0.2}$), agreeing with the LESR densities [5-7]. These results support also that LESR reflects photocarriers localized in band-tail states, which subsequently recombine to give the long-lasting PL decay.

Moreover, as G decreases below ~10^{16} cm^{-3}s^{-1}, n_{met} (×) as well as the LESR results deviates from the sub-linear dependence of $G^{0.2}$, with the deviation being larger for the defective a-Si:H (+) shown in Fig. 4. Actually, the PL decay curve of the defective film (plotted in half-tone) deviates more pronouncedly from the asymptotically converged curves at $t \approx 10^3$ s (Fig. 6). Non-radiative recombination at the defect sites probably participates in shortening the fate of metastable carriers, since n_{met} becomes comparable with the defect density (Fig. 5) [19,35,36].

4. Effect of electric field on geminate recombination and non-geminate (DP) recombination

The effect of a magnetic field of 0.9 T on the PL lifetime distribution was studied on a-Si:H [23] and a-As_2Se_3 [16]. Application of the magnetic field to both materials weakened the DP recombination component and enhanced the triplet-exciton component, whereas it did not affect the singlet-exciton component. The quenching of the DP component was interpreted in terms of the paramagnetism of DP carriers. The enhancement of the triplet exciton component was explained by the Zeeman interaction due to $S = 1$ for the triplet exciton; the singlet exciton has no Zeeman interaction because $S = 0$, thereby being unaffected by the magnetic field.

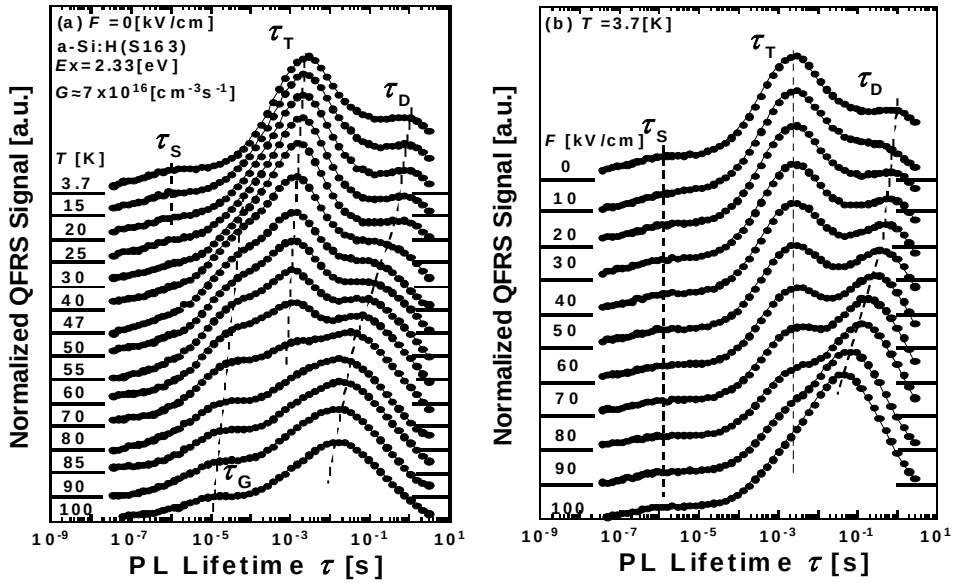

Fig. 8(a) T- evolved QFRS spectra of a-Si:H at F = 0 kVcm^{-1}. (b) F- evolved QFRS spectra of the same sample of (a) at T = 3.7K. PL was excited at E_X = 2.33 eV and G ≈ 7 × 10^{16} cm^{-3}s^{-1} in both (a) and (b)[21].

The effect of an electric field F (≤ 100 kVcm^{-1}) on the QFRS spectrum of the PL in a-Si:H was investigated in [21,22]. Figures 8(a) and (b) demonstrate the T-evolved QFRS spectra of the PL in a-Si:H at F = 0 kVcm^{-1} and the F-evolved spectra at T = 3.7 K, respectively, both under the geminate condition ($G \approx 7 \times 10^{16}$ cm^{-3}s^{-1}) [21].

Roughly speaking, the effects of temperature and electric field resemble each other; increasing either T or F reduces the excitonic components, but enhances the DP component. However, a crucial difference between Figs. 8(a) and (b) is the appearance of a new lifetime (τ_G) component between τ_S and τ_T above T = 25 K in Fig. 8(a). This has already been explained by the formation of geminate e-h pairs; as T rises above 25 K, excitation of thermal phonons prevents photogenerated e-h pairs from forming excitons, whereas non-excitonic, i.e., spin-free geminate pairs can be formed instead [15,20].

Since an electric field does not induce the phonon excitation, the electric field quenching of the excitonic or geminate component at low T has been explained in terms of the F-induced dissociation of excitons or geminate e-h pairs by various authors [3, 37-40].

In contrast to the excitonic or geminate component, however, we can see the shortening of the lifetime τ_D as well as the enhancement of the DP component with increasing T (Fig. 8(a)) and with increasing F (Fig. 8(b)). The DP lifetime τ_D is shortened by almost 2 orders of magnitude in the PL of undoped a-Si:H subjected to a strong electric field up to 100 kVcm^{-1} at T = 3.7 K.

The shortening of the lifetime τ_D accompanied by the enhancement of the QE η_D with increasing T cannot be explained by the competition with non-radiative recombination, e.g. due to thermally-excited phonons. This temperature effect on the DP component is interpreted in terms of increasing the number of recombination paths as well as the hopping diffusion, due to the hop-up of electrons localized in band-tail states by elevated T [35]. This is supported by the enhancement of η_D and shortening of τ_D by superposing infrared (IR) light in the PL of a-Si:H; it enhanced not only the DP recombination but also photoconductivity (PC), i.e., the hopping transport of a-Si:H at low T [13,40].

In a strong electric field at T = 0, an electron can increase its energy with respect to the mobility edge by hopping over a distance against the electric field. This is analogous to an activation at a finite, or *effective* temperature T, and thus F plays a role similar to T for the hopping conduction [41]. The interplay between the T- and F-dependences of the lifetime τ_D is interpreted on the basis of the *effective temperature* theory developed for the high-field hopping transport of charge carriers in disordered materials at low T [21,35,41].

The proportionality factor between T- and F-dependences of τ_D is ~ 0.6, which is close to that obtained from those of the transport coefficients [21]. Our experimental results, therefore, prove that the DP recombination event is closely connected to the transport phenomena in a-Si:H as predicted by the theory based on the photocarriers localized in band-tail states [35].

5. Summary

The triple-peaked lifetime distribution obtained by wideband QFRS reveals that PL in a-Si:H at low T and low G originates from both excitonic recombination and DP recombination. The triple-peaked lifetime distribution has been universally observed in amorphous

chalcogenides as well as tetrahedrally-bonded amorphous semiconductors.

The steady-state carrier density of the DP component in the QFRS spectra agrees with the LESR density in the *G*- and *T*-dependences in a-Si:H. The residual PL decay observed up to $t > 10^4$ s shows striking similarities to the LESR results in the *G*-dependences of the metastable carrier density and the two fitting parameters of the SE function, supporting the conclusion that the DP component and the LESR signal share common origins.

Application of an electric field to a-Si:H decreases the excitonic recombination by field-induced exciton dissociation, while it enhances the DP recombination. The latter is interpreted in terms of the *effective temperature* theory for the photocarriers localized in band-tail states.

Acknowledgements

The author would like to express his gratitude to the Chairman Acad. A. G. Petrov and all of the organisers of the 15th ISCMP for awarding him the Georgi Nadjakoff Memorial Lecture.

He also wishes to thank all of his colleagues; S. Komedoori, T. Shimizu, K. Ikeda, D. Saitou, N. Ohrui, S. Ishii, S. Kobayashi and C. Fujihashi of Tokyo Polytechnic University, A. Ganjoo and K. Shimakawa of Gifu University, J. Singh of Charles Darwin University, C. Koughia and S. O. Kasap of University of Saskatchewan for their valuable contributions to this work. Acknowledgement also is due to Professor Emeritus K. Morigaki for providing an important preprint [34].

The work was financially supported in part by the Japan Private School Promotion Foundation and by a Grant-in-Aid for Scientific Research (C) from the Ministry of Education, Culture, Sport, Science and Technology of Japan.

References

[1] T. Aoki, Optical Properties of Condensed Matter and Applications, ed. J. Singh, John Wiley & Sons, Chichester (2006), p.75.
[2] C. Tsang, R. A. Street, Phys. Rev. **B19**, 3027 (1979).
[3] D. Engemann, R. Fischer, Structure and Excitations of Amorphous and Liquid Semiconductors, ed. G. Lucovsky and F.L. Galeener, AIP, New York (1976), p.37.
[4] R. A. Street, Philos. Mag. **B37**, 35 (1978).
[5] M. Bort, W. Fuhs, S. Liedtke, R. Stachowitz, R. Carius, Philos. Mag. Lett. **64**, 227 (1991).
[6] F. Boulitrop, D. L. Dunstan, Solid State Common. **44**, 841 (1982).
[7] B. Yan, N. A. Schultz, A. L. Efros, P.C. Taylor, Phys. Rev. Lett. **84**, 4180 (2000).
[8] D .J. Dunstan, Philos. Mag. **B52**, 111 (1985).
[9] F. Boulitrop, D. J. Dunstan, J. Non-Cryst. Solids **77**&**78**, 663 (1985).
[10] S. Ambros, R. Carius, H. Wagner, J. Non-Cryst. Solids **137**&**138**, 555 (1991).
[11] R. Stachowitz, M. Schubert, W. Fuhs, J. Non-Cryst. Solids **227-230**, 190 (1998).
[12] S. Ishii, M. Kurihara, T. Aoki, K. Shimakawa, J. Singh, J. Non-Cryst. Solids **266-269**, 721 (2000).
[13] T. Aoki, K. Ikeda, N. Ohrui, S. Kobayashi, K. Shimakawa, J. Optoelectron. Adv. Mat. **9**, 70 (2007).
[14] T. Aoki, S. Komedoori, S. Kobayashi, T. Shimizu, A. Ganjoo, K. Shimakawa, J. Non-Cryst. Solids **326** & **32**7, 273 (2003).
[15] T. Aoki, T. Shimizu, S. Komedoori, S. Kobayashi, K. Shimakawa, J. Non-Cryst. Solids **338-340**, 456 (2004).
[16] T. Aoki, D. Saitou, K. Ikeda, S. Kobayashi, K. Shimakawa, J. Optoelectron. Adv. Mat. **7**, 1749 (2005).
[17] T. Aoki, D. Saitou, S. Kobayashi, C. Fujihashi, K. Shimakawa, M. Munzar, K. Koughia, S. O. Kasap, J. Mat. Sci. Mat. Electron. **18**, S97 (2007).
[18] T. Aoki, D. Saitou, S. Kobayashi, C. Fujihashi, K. Shimakawa, M. Munzar, K. Koughia, S.O. Kasap, J. Optoelectron. Adv. Mat. **9**, 3143 (2007).
[19] T. Aoki, K. Ikeda, S. Kobayashi, K. Shimakawa, Philos. Mag. Lett. **86**, 137 (2006).
[20] T. Aoki, J. Non-Cryst. Solids **352**,1138 (2006).
[21] T. Aoki, N. Ohrui, C. Fujihashi, K. Shimakawa, Philos. Mag. Lett. **88**, 9 (2008).
[22] T. Aoki, N. Ohrui, C. Fujihashi, K. Shimakawa, J. Mat Sci. Mat. Electron. (2008) *in press*.
[23] T. Aoki, T. Shimizu, D. Saitou, K. Ikeda, J. Optoelectron. Adv. Mat. **7**, 137 (2005).
[24] T. Aoki, S. Komedoori, S. Kobayashi, T. Shimizu, A. Ganjoo, K. Shimakawa, Nonlinear Optics **29**, 273 (2002).
[25] T. Aoki, J. Mat. Sci. Mat. Electron. **14**, 697 (2003).
[26] N. F. Mott, Philos. Mag. **36**, 413 (1977).
[27] S. Kivelson, C. D. Gellat Jr., Phys. Rev. **B26**, 4646 (1982).

[28] E. Davis, Amorphous Semiconductors, ed. M.H. Brodsky, Springer-Verlag, Berlin (1979), p.41.
[29] B. A. Wilson, P.Hu, T.M. Jedju, J.P. Harbison, Phys. Rev. **B28**, 5901 (1983).
[30] J. Singh, I.-K. Oh, J. Appl. Phys. **97**, 063516 (2005).
[31] J. Singh, Phys. Rev. **B76**, 085205 (2007).
[32] D. G. Stearns, Phys. Rev. **B30**, 6000 (1984).
[33] J. Singh, T. Aoki, K. Shimakawa, Phil. Mag. **B82**, 855 (2002).
[34] K. Morigaki, to be published in phys. stat. sol. (c).
[35] B. I. Shkolvskii, E. I. Levine, H. Fritzsche, S. D. Baranovskii, in Transport, Correlation and Structural Defects, ed. H. Fritzsche, World Scientific, Singapore (1990), p.161.
[36] D. J. Dunstan, Philos. Mag. **B49**, 191 (1984).
[37] J. I. Pankove, D. E. Carlson, Appl. Phys. Lett. **29**, 620 (1976).
[38] T. S. Nashashibi, I. G. Austin, T. M. Searle, Proc. 7th Int. Conf. on Amorphous and Liquid Semiconductors, ed. by W. E. Spear, CICL, Edinburgh (1977), p.392.
[39] M. A. Paesler, W. Paul, Philos. Mag. **B41**, 393 (1980).
[40] R. Carius, W. Fuhs, A. Schrimpf, in Tetrahedrally-Bonded Amorphous Semiconductors, ed. D. Adler and H. Fritzsche, Plenum Press, New York (1985), p.367.
[41] B. I. Shklovskii, Soviet Phys. Semicond. **6**, 1964 (1973).

*Corresponding author: aoki@ee.t-kougei.ac.jp